

Creation of a three-dimensional printed spine model for training in pain procedures

Journal of International Medical Research

49(11) 1–14

© The Author(s) 2021





Article reuse guidelines:

sagepub.com/journals-permissions

DOI: 10.1177/03000605211053281

journals.sagepub.com/home/imr



Jae Chul Koh¹ , Yoo Kyung Jang¹ ,
Hyunyoung Seong¹ , Kae Hong Lee¹,
Seungwoo Jun¹ and Jong Bum Choi² 

Abstract

Objective: Technological developments have made it possible to create simulation models to educate clinicians on surgical techniques and patient preparation. In this study, we created an inexpensive lumbar spine phantom using patient data and analyzed its usefulness in clinical education.

Methods: This randomized comparative study used computed tomography and magnetic resonance imaging data from a single patient to print a three-dimensional (3D) bone framework and create a mold. The printed bones and structures made from the mold were placed in a simulation model that was used to train residents. The residents were divided into two groups: Group L, which received only an audiovisual lecture, and Group P, which received an additional 1 hour of training using the 3D phantom. The performance of both groups was evaluated using pretest and post-test analyses.

Results: Both the checklist and global rating scores increased after training in both groups. However, some variables improved significantly only in Group P. The overall satisfaction score was also higher in Group P than in Group L.

Conclusions: We have described a method by which medical doctors can create a spine simulation phantom and have demonstrated its efficiency for procedural education.

¹Department of Anesthesiology and Pain Medicine, Korea University Anam Hospital, Seoul, Korea

²Department of Anesthesiology and Pain Medicine, Ajou University Hospital, Suwon, Korea

Corresponding author:

Jong Bum Choi, Department of Anesthesiology and Pain Medicine, Ajou University Hospital, 164 World Cup-ro, Yeongtong-gu, Suwon 16499, Korea.
Email: romeojb@naver.com



Keywords

Autonomic nerve block, epidural anesthesia, high-fidelity simulation training, lumbar vertebra, magnetic resonance imaging, phantom, imaging, printing, three-dimensional, simulation training

Date received: 9 May 2021; accepted: 21 September 2021

Introduction

The incidence of spinal degenerative disease is increasing with the aging of the general population.¹ The development and implementation of fluoroscopic-guided procedures for patients with spinal degenerative disease have contributed to improved treatments and symptom management.² Ultrasound techniques may be used for these procedures, eliminating the risk of radiation exposure; however, the difficulty in predicting drug distributions using contrast agents and in determining the exact structure of the bones makes fluoroscopy difficult to replace.³ Although cadaver workshops and simulation models have been used to teach infiltration techniques,⁴ supplying cadavers is challenging and the price of simulation models is high, making it difficult to easily use these teaching methods. Moreover, manufactured phantoms often do not sufficiently satisfy the needs of clinicians, and there are many restrictions on their use in advanced practice involving difficult cases.

Recent price reductions and the popularization of three-dimensional (3D) printers have provided a convenient way to produce many models and tools at a reasonable price with easy accessibility.^{5,6} In addition, the transformation of medical images, including those from computed tomography (CT) or magnetic resonance imaging scans, into a 3D printable format has become more attainable.⁷ These techniques allow the creation of simulation models for learning as well as for preparing patients

before difficult procedures at a reasonable price.^{8,9}

Several studies have demonstrated the efficacy of using phantoms to teach procedures.^{5,8,10–13} However, to the best of our knowledge, this is the first study to evaluate the efficacy of simulation phantoms for training in the performance of selective transforaminal epidural block (STEB), medial branch block (MBB), and lumbar sympathetic ganglion block (LSGB) procedures. In addition, standard tools to evaluate the learning effects of these procedures are lacking.

Therefore, we developed an inexpensive, clinician-made lumbar spine phantom using patient data and analyzed its effectiveness in teaching STEB, MBB, and LSGB procedures on the lumbar spine.

Materials and methods

Simulation phantom creation

Segmentation and polygonization. Patient lumbar CT and magnetic resonance images were obtained from the anonymized data server in Digital Imaging and Communications in Medicine (DICOM) format. 3D Slicer version 4.10.2 (<http://www.slicer.org>) was used for image segmentation. First, volumetric medical images of a target vertebra, sacrum, and pelvic bone were acquired by setting a threshold range of intensity. However, because of data limitations such as the heterogeneity of the bone intensity and low resolution of the

CT slices, it was difficult to precisely determine the vertebral structure, especially that of the articular processes at the boundary between adjacent vertebrae. Therefore, one doctor (JC Koh) used his anatomical knowledge to carefully compare and analyze multiple CT views (axial, coronal, and sagittal) to manually determine the precise anatomical structure. Moreover, it was also difficult to accurately separate the intervertebral disc from other structures based on the CT images alone. Because CT data comprise a set of Hounsfield units, the differences between the intervertebral disc and surrounding muscle or fat tissue were not clear. Therefore, magnetic resonance images were used to better visualize the shape of the intervertebral discs. After segmentation, the surface mesh data of the vertebrae and pelvic bone consisted of 60,000 to 80,000 triangles each, while the

sacrum contained more than 110,000 such triangles. To shorten the printing time and increase efficiency, the number of polygons was reduced to 10% of the original mesh data using Meshmixer version 3.5 (Autodesk Inc., San Rafael, CA, USA) in preparation for 3D printing (Figure 1).

Bone and intervertebral disc generation. The vertebrae and pelvic bones were printed directly using a 3D printer (CR-10; Creality 3D, Shenzhen, China). For the best performance, the bone inner density was set to 90% after a series of pretests using a C-arm (Figure 2(a)). The printing was performed with fused deposition modeling using a polylactic acid filament. To make the intervertebral discs invisible by X-ray, the frame was constructed first. Polyurethane foam was then injected into this frame to completely fill and provide

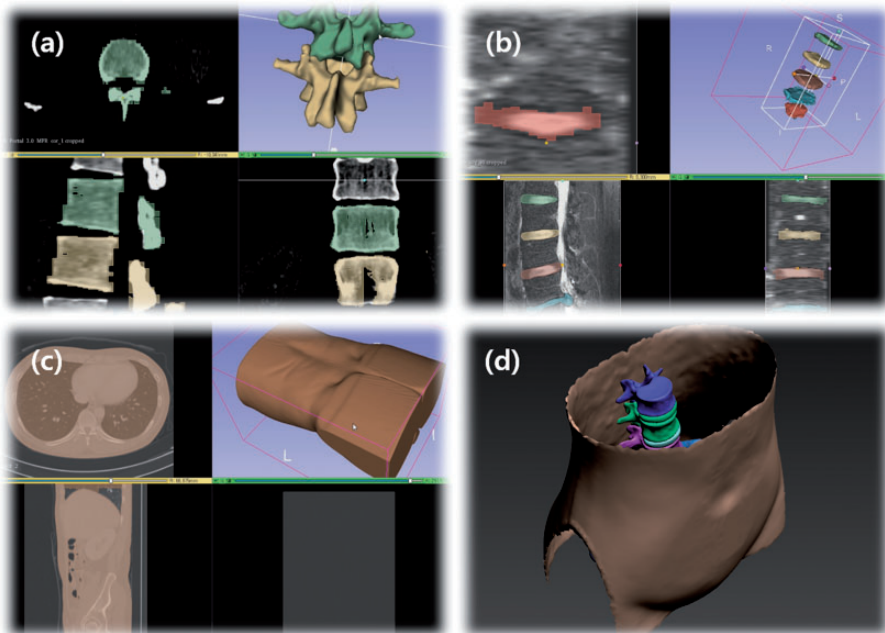


Figure 1. Segmentation of the vertebrae and pelvic bone, intervertebral discs, and body contour using the 3D Slicer software package applied to computed tomography (CT) and magnetic resonance imaging data. (a) Vertebrae and pelvic bone from CT. (b) Intervertebral discs from magnetic resonance imaging. (c) Body contour from CT. (d) Combined surface mesh data.

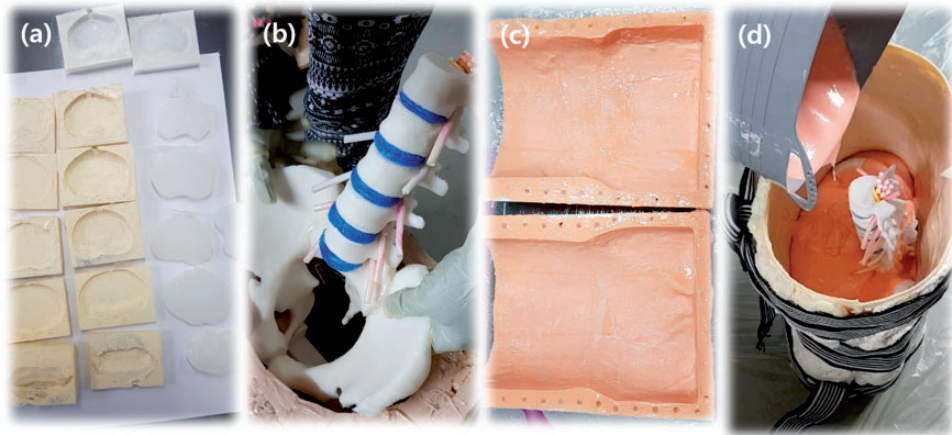


Figure 2. Vertebrae and pelvic bone were assembled after printing. The intervertebral discs and body contour were printed first and used to make a mold. (a) Molds for intervertebral discs. (b) Assembled vertebral bones and intervertebral discs. (c) Silicone layer applied to the body contour mold. (d) Polyurethane foam injected to the mold.

the precise shape of the mold (Figure 2(b)). Two board-certified doctors with more than 10 years of experience in analyzing and interpreting image data in clinical practice carefully compared the resulting printed bones and intervertebral disc structures with the original CT and magnetic resonance imaging data.

Skin and muscle generation. Before building the phantom model, numerous materials were tested to best mimic human skin and muscle. Several materials were tested to identify those that most closely reproduced the feeling of the patient's skin, including VytaFlex 10, Ecoflex 0010, Ecoflex 0020, Ecoflex 0030, and Ecoflex 0035 (Smooth-On Inc., Macungie, PA, USA). We applied approximately 0.5 cm of each material to the surface of a polyurethane foam mass to form the skin. Six doctors experienced in intervention procedures were then asked to puncture the skin material with a 22-gauge spinal needle. Among these materials, four doctors reported that Ecoflex 0030 felt closest to human skin puncture, whereas one doctor each reported that

Ecoflex 0035 and Ecoflex 0020 felt closest. After a series of tests using X-rays, we found that a sufficiently thin synthetic skin layer did not affect the overall radiologic simulation while sufficiently mimicking the tactile and physical properties of human skin. Thus, Ecoflex 0030 was determined to most closely resemble human skin and was finally selected.

To generate the muscles used in the phantom, we sought to identify a material with a texture resembling that of muscles and with a radiolucent property that would allow visualization of bones or instruments during X-ray-guided procedures. The candidate materials were Ecoflex 0020, Ecoflex 0030, FlexFoam-iT! III, and FlexFoam-iT! V (Smooth-On Inc.). Each material was produced as a mass containing a 3D-printed vertebra. X-ray images were then taken to assess these materials. Among them, only FlexFoam-iT! III and V provided satisfactory X-ray images; the other materials absorbed X-rays. Although these two polyurethane foam materials had similar tactile and radiologic features, FlexFoam-iT! III was easier to process;

thus, it was selected as the material most closely resembling human muscle.

After choosing the final materials for building the skin and muscles, the body contour was printed as a mold. After thorough application of a coating of silicone release agent, Ecoflex 0030 was applied to the inner surface of the printed body mold. To achieve satisfactory skin with homogeneous thickness, the whole mold was rotated in several directions until the silicone solidified. The assembled bones and intervertebral discs were then inserted into the mold (Figure 2(c)). The final phantom model was developed by pouring the muscle-mimicking material into the mold and drying it (Figure 2(d)).

After producing the phantom, two experienced doctors performed the X-ray-guided procedures using the phantom

and confirmed their satisfaction with the model (Figure 3).

Validation

This prospective, randomized study was approved by the Institutional Review Board of Korea University Anam Hospital, Seoul, Republic of Korea (approval no. 2019AN0237, approval date 10 June 2019) and was registered in the Clinical Research Information Service (<http://cris.nih.go.kr>; registration no. KCT0004684). Twelve anesthesiology and pain medicine residents participated in the validation of the phantom. After providing written informed consent, these participants were randomly assigned to either the audiovisual lecture group (Group L) or the phantom training group (Group P).

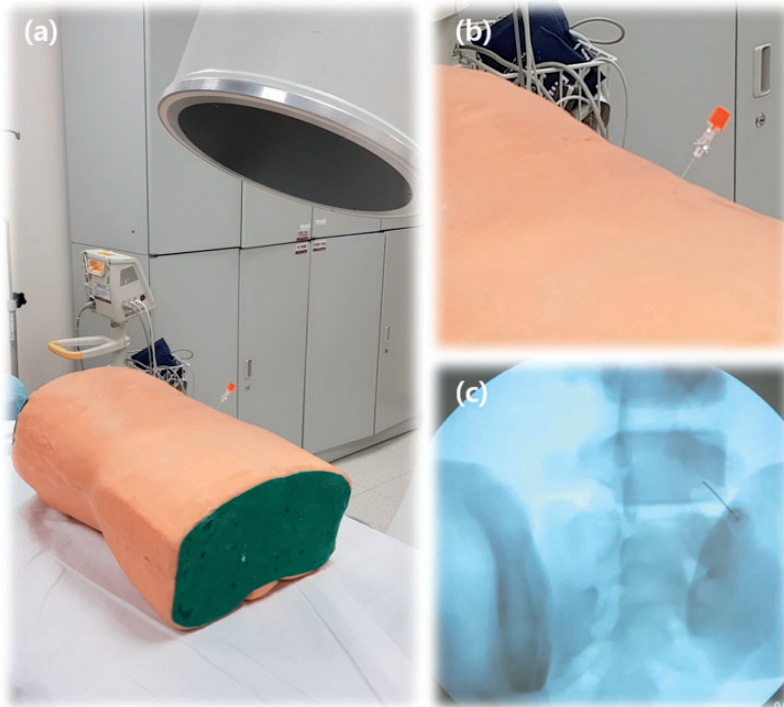


Figure 3. Completed simulation phantom model and assessment. (a) Completed phantom model with C-arm. (b) The model with insertion of a 22-gauge needle. (c) C-arm image of the model and needle.

Pretest analysis

The participants' sex, age, and resident training year were requested and recorded. Information on their previous experiences with observing, assisting, and performing the procedures was also obtained. First, all participants were instructed to perform STEB, MBB, and LSGB using a spine phantom with no explanation beforehand. The procedures were performed at the following levels: STEB was performed through the intervertebral foramen between L5 and the sacrum, MBB targeted the nerve traversing the L4 transverse process, and LSGB targeted the sympathetic ganglion near the anterior L3 lower body. The global rating score, checklist score, procedure duration, and number of C-arm images taken were measured by two board-certified pain medicine physicians. The average scores calculated by two examiners with more than 10 years of clinical experience (JC Koh and JB Choi) were used for the assessment. We used the checklist score developed by Gonzalez-Cota et al.⁸ for STEB. Because we found no assessment tools for MBB and LSGB, we developed checklist scores for these procedures by modifying the checklist score used for STEB. The checklist scores were translated into Korean (Appendix 1). The global rating score created by Gonzalez-Cota et al.⁸ and Reznick et al.¹⁴ was applicable to all three procedures without any modification except for translation (Appendix 2).

The procedure duration was measured from the time at which the first C-arm image was taken until the time at which the drug was administered.

Training

The participants in both groups received a 1-hour lecture using audiovisual material to teach the STEB, MBB, and LSGB procedures. Additionally, the participants in

Group P received an extra 1-hour session during which they could practice using the simulation phantom.

Post-test analysis

The post-test analysis was similar to the pretest analysis. However, the rate of overall satisfaction with the education was evaluated on a 5-point Likert scale (1 = very unsatisfied, 5 = very satisfied).

Statistical analysis

The sample size was calculated using NCSS 12 Statistical Software (NCSS, LLC, Kaysville, UT, USA). The minimum effect size of each score used in the calculation was based on the results reported by Gonzalez-Cota et al.⁸ The results of these calculations showed a minimum of five required patients. Assuming a dropout rate of 10%, a minimum recruitment requirement of six participants per group was calculated.

Statistical analysis was performed using SAS version 9.4 (SAS Institute Inc., Cary, NC, USA) and IBM SPSS Statistics for Windows, version 25.0 (IBM Corp., Armonk, NY, USA). The results are expressed as mean \pm standard deviation, median (interquartile range), or number of participants. Because the variables in each group were not normally distributed, we conducted Fisher's exact test or the Mann-Whitney U test to compare demographics and prior experiences between the groups. The Mann-Whitney U test and Wilcoxon signed-rank test were used to compare pretest and post-test period parameters in the two groups. Intraclass correlation coefficients were used to measure the reliability of the checklist and global rating scale.

Results

Twelve residents (8 men, 4 women) participated in this study. Their demographic

characteristics and prior experiences are presented in Table 1. There were no significant differences between the groups.

Table 2 presents the medians and interquartile ranges of the pretest and post-test results of STEB, including the checklist and global rating scores, procedure duration, and number of C-arm images taken. Group P showed significantly improved global rating scores (post-pre score = 14.5, $P=0.031$) and a decreased procedure time (post-pre seconds = -107.0, $P=0.031$), whereas the changes were not significant in Group L. The checklist scores and number of C-arm images did not significantly change in either group.

The results for MBB are presented in Table 3. Both the audiovisual lecture and phantom training helped to improve the checklist scores ($P=0.031$ for both); however, only phantom training significantly improved the global rating scores (post-pre score = 10.5, $P=0.031$), with a lower number of C-arm images required (post-pre number = -7.0, $P=0.031$). However, the procedure duration decreased

significantly in Group L (post-pre seconds = -47.0, $P=0.031$).

Table 4 presents the results for LSGB. Phantom training helped to increase both the checklist and global rating scores (post-pre checklist score = 3.5, $P=0.031$; post-pre global rating score = 10.3, $P=0.031$), whereas the changes were not significant in Group L. The procedure time significantly decreased in Group P (post-pre seconds = -82.0, $P=0.031$) without a change in the number of C-arm images.

The mean values of the checklist and global rating score results are presented in Figure 4. In all techniques, the post-test mean scores increased in both groups; however, the slope tended to be steeper in Group P, indicating a more prominent improvement in technique with phantom training in a short duration of training time, regardless of the type of technique. In other words, phantom training might help trainees to easily acquire clinical skills.

The participants in Group P showed a higher overall satisfaction score than the

Table 1. Participants' demographics and prior experience.

Parameters	Group L (n = 6)	Group P (n = 6)	P-value
Sex, male/female	4/2	4/2	>0.999
Resident training year, II/III/IV	2/3/1	3/1/2	0.610
Age, years	30.5 [28.0, 36.0]	34.5 [28.0, 36.0]	0.753
Prior observation			
STEB	10.0 [1.0, 15.0]	10.0 [5.0, 15.0]	>0.999
MBB	10.0 [1.0, 15.0]	10.0 [5.0, 15.0]	>0.999
LSGB	3.0 [0.0, 15.0]	5.0 [5.0, 10.0]	0.747
Prior assistance			
STEB	7.5 [1.0, 15.0]	6.0 [2.0, 15.0]	>0.999
MBB	7.5 [1.0, 15.0]	6.0 [2.0, 15.0]	>0.999
LSGB	1.0 [0.0, 15.0]	3.5 [2.0, 10.0]	0.693
Prior performance			
STEB	1.0 [0.0, 10.0]	1.5 [1.0, 10.0]	0.574
MBB	1.0 [1.0, 10.0]	1.5 [1.0, 10.0]	0.744
LSGB	0.0 [0.0, 1.0]	1.0 [1.0, 2.0]	0.230

Data are shown as number of participants or median [interquartile range].

STEB, selective transforaminal epidural block; MBB, medial branch block; LSGB, lumbar sympathetic ganglion block.

Table 2. Pretest and post-test results for selective transforaminal epidural block.

Parameters	Group L (n = 6)	Group P (n = 6)	P-value
Checklist score (0–7)			
Pre	0.8 [0.0, 4.5]	2.5 [1.0, 4.0]	0.752
Post	4.5 [4.0, 6.0]	5.0 [5.0, 6.5]	0.344
Post–pre	3.0 [0.5, 4.0]	2.8 [2.0, 5.0]	>0.999
P value	0.063	0.063	
Global rating score (7–35)			
Pre	8.3 [7.0, 21.5]	13.0 [7.0, 17.0]	0.935
Post	21.3 [14.0, 23.5]	27.0 [24.5, 29.5]	0.081
Post–pre	7.8 [3.0, 14.0]	14.5 [7.5, 22.0]	0.200
P value	0.063	0.031*	
Procedure duration, seconds			
Pre	286.0 [225.0, 359.0]	251.0 [219.0, 412.0]	0.815
Post	214.0 [137.0, 338.0]	160 [157.0, 172.0]	0.440
Post–pre	–53.0 [–84.0, –15.0]	–107.0 [–240.0, –44.0]	0.254
P value	0.063	0.031*	
Number of C-arm images taken			
Pre	12.5 [8.0, 23.0]	14.0 [12.0, 15.0]	0.695
Post	16.5 [8.0, 21.0]	12.5 [7.0, 15.0]	0.395
Post–pre	–0.5 [–1.0, 2.0]	–2.0 [–8.0, 1.0]	0.639
P value	>0.999	0.313	

Data are shown as median [interquartile range].

*P < 0.05.

Table 3. Pretest and post-test results for medial branch block.

Parameters	Group L (n = 6)	Group P (n = 6)	P-value
Checklist score (0–7)			
Pre	2.5 [0.5, 3.0]	2.5 [1.0, 3.0]	>0.999
Post	4.0 [4.0, 5.0]	5.0 [5.0, 6.0]	0.090
Post–pre	2.0 [1.0, 3.0]	2.5 [2.0, 5.0]	0.388
P value	0.031*	0.031*	
Global rating score (7–35)			
Pre	11.8 [9.0, 22.0]	14.8 [7.0, 20.0]	0.937
Post	24.0 [17.0, 28.0]	25.0 [23.0, 30.0]	0.439
Post–pre	8.5 [8.0, 14.0]	10.5 [2.0, 19.0]	0.696
P value	0.063	0.031*	
Procedure duration, seconds			
Pre	211.0 [157.0, 311.0]	194.0 [131.0, 380.0]	0.938
Post	145.5 [128.0, 207.0]	147.5 [129.0, 169.0]	0.938
Post–pre	–47.0 [–108.0, –18.0]	–55.0 [–239.0, –9.0]	0.815
P value	0.031*	0.156	
Number of C-arm images taken			
Pre	11.5 [9.0, 21.0]	14.0 [12.0, 22.0]	0.585
Post	11.0 [9.0, 17.0]	10.0 [6.0, 12.0]	0.531
Post–pre	–2.0 [–10.0, –1.0]	–7.0 [–10.0, –4.0]	0.437
P value	0.219	0.031*	

Data are shown as median [interquartile range].

*P < 0.05.

Table 4. Pretest and post-test results for lumbar sympathetic ganglion block.

Parameters	Group L (n = 6)	Group P (n = 6)	P-value
Checklist score (0–7)			
Pre	0.8 [0.0, 3.0]	2.0 [1.0, 2.0]	0.692
Post	4.0 [3.0, 5.0]	6.0 [4.0, 7.0]	0.214
Post–pre	2.0 [2.0, 3.0]	3.5 [2.0, 6.0]	0.411
P value	0.063	0.031*	
Global rating score (7–35)			
Pre	7.8 [7.0, 21.0]	10.5 [7.0, 16.5]	0.935
Post	21.0 [15.0, 23.5]	22.3 [18.5, 29.5]	0.439
Post–pre	8.0 [1.0, 12.5]	10.3 [4.0, 21.0]	0.397
P value	0.063	0.031*	
Procedure duration, seconds			
Pre	278.5 [182.0, 354.0]	254.5 [225.0, 292.0]	0.754
Post	221.5 [150.0, 289.0]	160.0 [140.0, 176.0]	0.255
Post–pre	–33.5 [–57.0, 43.0]	–82.0 [–177.0, –49.0]	0.201
P value	0.563	0.031*	
Number of C-arm images taken			
Pre	16.0 [15.0, 21.0]	17.0 [14.0, 20.0]	>0.999
Post	18.5 [14.0, 29.0]	13.0 [11.0, 15.0]	0.251
Post–pre	–3.0 [–7.0, 18.0]	–6.0 [–9.0, –2.0]	0.486
P value	>0.999	0.156	

Data are shown as median [interquartile range].

* $P < 0.05$.

participants in Group L (5.0 [4.0, 5.0] vs. 3.0 [3.0, 3.0], $P = 0.017$). The results of the interobserver reliability assessment are shown in Table 5. The values were >0.8 for all tests, indicating a high degree of interobserver agreement.

Discussion

We successfully created a procedure simulation model using patient DICOM data and a 3D printer. Using the simulation model for training helped to teach various spinal procedures, including STEB, MBB, and LSGB.

The simulation phantom created in this study replicated, as closely as possible, the actual size and structure of the spine based on DICOM data from a real patient. Unlike other commercial models, the phantom created in this study was developed from segmentation to manufacturing by a

doctor (JC Koh) who diagnoses and treats actual patients to provide the most suitable structure and function for the procedure performance. In clinical practice CT of the spine generally has wide cuts and low resolution to reduce the patient's radiation dose and examination time. In addition, because most patients undergoing spinal surgeries are of advanced age, degenerative changes in these patients affect the anatomical structures as well as the homogeneity of the bone density,¹⁵ making segmentation more difficult. In young patients, the facet joint between the superior and inferior articular processes is often wide enough and the vertebral body can be more easily separated from the intervertebral disc. However, these gaps become narrow in older patients, and changes in bone density due to osteoporosis are often accompanied by calcification of the intervertebral discs, end plates, and facet joints. Various degenerative

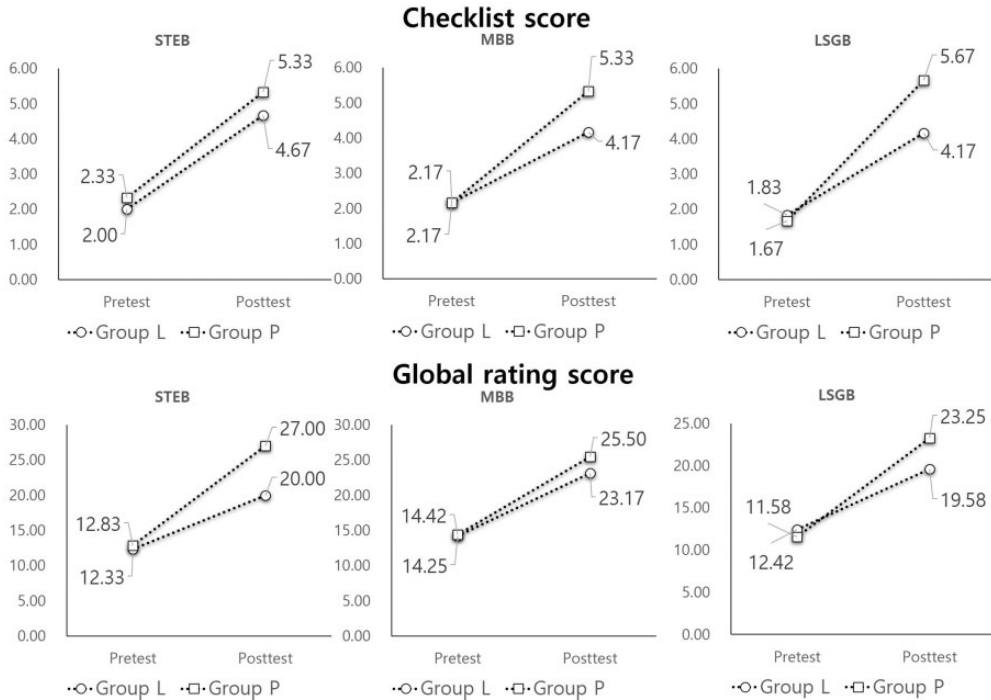


Figure 4. Changes in mean checklist and global rating scores in both groups. The post-test scores were higher than the pretest scores in both groups. STEB, selective transforaminal epidural block; MBB, medial branch block; LSGB, lumbar sympathetic ganglion block.

Table 5. Intraobserver reliability.

Parameters	STEB	MBB	LSGB
Pretest			
Checklist score	0.982 [0.910, 0.995]	0.967 [0.891, 0.991]	0.978 [0.926, 0.994]
Global rating score	0.994 [0.980, 0.998]	0.991 [0.970, 0.997]	0.998 [0.993, 0.999]
Post-test			
Checklist score	0.940 [0.806, 0.982]	0.861 [0.587, 0.958]	0.949 [0.833, 0.985]
Global rating score	0.996 [0.986, 0.999]	0.989 [0.963, 0.997]	0.996 [0.988, 0.999]

Data are shown as intraclass correlation coefficient [95% confidence interval].

STEB, selective transforaminal epidural block; MBB, medial branch block; LSGB, lumbar sympathetic ganglion block.

changes such as Modic changes, Schmorl’s nodes, or erosions can also prevent accurate segmentation. Although various methods have been studied and developed to overcome the difficulties of spinal segmentation, these methods have many limitations in terms of cost and accessibility.^{16,17}

However, if the physician performing the procedure also performs the segmentation and polygonization, as in this study, an inexpensive and more accurate 3D model can be produced using anatomical knowledge with a focus on the relevant structures. In addition, without adequate medical

knowledge, it is difficult to reflect the difficulties generated by these changes that need to be carefully considered in performing these procedures.

After several rounds of trial and error, we identified skin and muscle materials that most accurately reproduced the feeling of needle insertion and created realistic X-ray images. Our production process is useful not only for education but also for the simulation of procedures when difficult cases are anticipated. Even experienced operators may encounter difficulty applying the desired surgical tools to the exact location on a 3D structure based on 2D images. Before performing the procedures on actual patients, practicing on a phantom will assist in gaining an accurate understanding of how 2D images reflect 3D structures.

Previous studies of lumbar procedures often reconstructed the lumbar vertebrae and sacral bones but not the pelvic bones, unlike in the present study.^{8,11} During spinal procedures, especially when performing STEB at the L5/S1 level, it is often difficult to identify the target point and secure the entry path of the needle because of the pelvic bone.¹⁰ Therefore, the phantom designed in the present study could also be useful for training and simulating transforaminal endoscopy or other procedures in which the pelvic bones may cause difficulty.

Spinal simulation phantoms have been reported to improve educational efficiency.^{8,11,12,18} However, previous studies did not compare the effectiveness of these phantoms in preparing for various procedures performed on the lumbar spine, as in the present study. Although such spinal procedures are widely performed, training evaluation is difficult because of the lack of performance assessment tools. In this study, we modified the scoring system described by Gonzalez-Cota et al.,⁸ which accurately assessed the efficacy of education for only STEB, to establish a scoring system for the educational efficacy of MBB and

LSGB. The results of this study showed interobserver reliability of at least 0.90 for all scores except the post-test checklist scores for MBB. Koo and Li¹⁹ defined intraclass correlation coefficients of >0.90 as excellent, while those of 0.75 to 0.90 were considered good. Therefore, although more research is needed, this scoring system may be useful for evaluating the training outcomes of spinal procedures.

Several studies have demonstrated the efficacy of using phantoms to teach different procedures.^{5,8,11-13} However, to our knowledge, this is the first study to evaluate the efficacy of simulation phantoms for the training of STEB, MBB, and LSGB.

In this study, most of the scores were higher in the post-test than pretest period, and the slope increase on the graph showing the average values was greater in Group P than in Group L. However, statistical significance was not obtained for many values. The main cause of this may have been the small sample size. Nevertheless, some items showed statistically significant changes. The post-test scores in Group P were significantly higher than the pretest scores despite the small sample size. This result may have been due to the more evident increase in post-training scores in Group P. Other studies have also demonstrated the effectiveness of phantoms, supporting the findings of the present study.^{5,8,11-13}

It is noteworthy that, unlike other results, the procedure time for MBB decreased in Group L. This was an unexpected result and may have been related to the small sample size and the difficulty of the procedure. Nevertheless, the decrease in the number of C-arm images taken and the increase in the global rating score were significant only in Group P. This difference might have resulted from the unsuccessful practicing of effective C-arm use in Group L. Some of the participants in Group L performed MBB without effectively rotating the C-arm to obtain a better view.

Therefore, although their procedures required less time, the procedure effectiveness and results were poorer. In contrast, participants in Group P adjusted the C-arm properly; although they required more time to rotate and position the C-arm, this proper adjustment led to greater procedural integrity.

Cohen et al.²⁰ reported that MBB can be performed with significantly lower radiation doses than those required for STEB or LSGB, indicating that the difficulty of MBB is relatively low. For STEB, accurate entry into the specified L5 intervertebral foramen target level may require considerable practice to avoid the pelvic bone and osteophytes of the transverse process in patients with a degenerative spine.²¹ LSGB may also require more practice. Because a large insertion depth is required to reach the target, it may be difficult to access the needle without changing the path to the target point or to pass near the vertebral body of a degenerative spine without damage. However, MBB requires the shortest path from the skin to the target point, and few structures are present to prevent entry; this may explain the lack of reduction in the procedure time after training using the phantom.

This study has several limitations. We were unable to achieve statistically significant results for many variables because of the small study population. In addition, despite having created a phantom enabling simulations that were very similar to those performed on real patients, we limited the study participants to residents. Therefore, we could not evaluate the similarity of touch, stiffness, or image quality to the actual procedures. However, we believe that the phantom development process, the considerations for its development, and the scoring systems used to evaluate the learning efficiency of procedures such as MBB and LSGB described in this study

will serve as excellent models for further studies.

In summary, we created a phantom for realistic simulation of fluoroscopic-guided procedures using DICOM data from a single patient. Training using this phantom was effective in teaching STEB, MBB, and LSGB and in reducing the procedure time and number of C-arm images taken. This phantom may be useful to simulate patients who are expected to undergo difficult procedures.

Acknowledgements

The authors thank Editage (www.editage.co.kr) for English language editing and Yujin Kwon at Ajou University Medical Information & Media Center for formatting of the paper.

Declaration of conflicting interest

The authors declare that there is no conflict of interest.

Funding


The authors disclosed receipt of the following financial support for the research, authorship, and publication of this article: Creation of the phantom produced in this study was financially supported by the Ministry of Trade Industry & Energy (MOTIE, Korea), the Ministry of Science & ICT (MSIT, Korea), and the Ministry of Health & Welfare (MOHW, Korea) under the Technology Development Program for AI-Bio-Robot-Medicine Convergence (20001655).


Author contributions


Jae Chul Koh: study planning and performance, data analysis, and manuscript writing. Yoo Kyung Jang, Hyunyoung Seong, Kae Hong Lee, Seungwoo Jun: study performance. Jong Bum Choi: study planning and performance, manuscript writing. All authors agreed to be accountable for all aspects of the work and approved the final manuscript as submitted.

ORCID iDs

Jae Chul Koh  <https://orcid.org/0000-0002-1625-8650>

Yoo Kyung Jang  <https://orcid.org/0000-0002-3491-1430>

Hyunyoung Seong  <https://orcid.org/0000-0001-5136-1058>

Jong Bum Choi  <https://orcid.org/0000-0003-2277-1095>

Supplemental material

Supplemental material for this article is available online.

References

- Fehlings MG, Tetreault L, Nater A, et al. The aging of the global population: The changing epidemiology of disease and spinal disorders. *Neurosurgery* 2015; 77 Suppl 4: S1–S5.
- Andreula C, Muto M and Leonardi M. Interventional spinal procedures. *Eur J Radiol* 2004; 50: 112–119.
- Wang D. Image guidance technologies for interventional pain procedures: Ultrasound, fluoroscopy, and CT. *Curr Pain Headache Rep* 2018; 22: 6.
- Michels NR and Vanhomwegen E. An educational study to investigate the efficacy of three training methods for infiltration techniques on self-efficacy and skills of trainees in general practice. *BMC Fam Pract* 2019; 20: 133.
- Cramer J, Quigley E, Hutchins T, et al. Educational material for 3D visualization of spine procedures: Methods for creation and dissemination. *J Digit Imaging* 2017; 30: 296–300.
- Garcia J, Yang Z, Mongrain R, et al. 3D printing materials and their use in medical education: A review of current technology and trends for the future. *BMJ Simul Technol Enhanc Learn* 2018; 4: 27–40.
- Zhang X, Xu Z, Tan L, et al. Application of three-dimensional reconstruction and printing as an elective course for undergraduate medical students: An exploratory trial. *Surg Radiol Anat* 2019; 41: 1193–1204.
- Gonzalez-Cota A, Chiravuri S, Stansfield RB, et al. The effect of bench model fidelity on fluoroscopy-guided transforaminal epidural injection training: A randomized control study. *Reg Anesth Pain Med* 2013; 38: 155–160.
- Provaggi E, Leong JJH and Kalaskar DM. Applications of 3D printing in the management of severe spinal conditions. *Proc Inst Mech Eng H* 2017; 231: 471–486.
- Joswig H, Haile SR, Hildebrandt G, et al. Residents' learning curve of lumbar transforaminal epidural steroid injections. *J Neurol Surg A Cent Eur Neurosurg* 2017; 78: 460–466.
- Mashari A, Montealegre-Gallegos M, Jeganathan J, et al. Low-cost three-dimensional printed phantom for neuraxial anesthesia training: Development and comparison to a commercial model. *PLoS One* 2018; 13: e0191664.
- Li Y, Li Z, Ammanuel S, et al. Efficacy of using a 3D printed lumbosacral spine phantom in improving trainee proficiency and confidence in CT-guided spine procedures. *3D Print Med* 2018; 4: 7.
- Faulkner AR, Bourgeois AC, Bradley YC, et al. Simulation-based educational curriculum for fluoroscopically guided lumbar puncture improves operator confidence and reduces patient dose. *Acad Radiol* 2015; 22: 668–673.
- Reznick R, Regehr G, MacRae H, et al. Testing technical skill via an innovative “bench station” examination. *Am J Surg* 1997; 173: 226–230.
- Parizel PM, Van Hoyweghen AJ, Bali A, et al. The degenerative spine: Pattern recognition and guidelines to image interpretation. *Handb Clin Neurol* 2016; 136: 787–808.
- Korez R, Ibragimov B, Likar B, et al. A framework for automated spine and vertebrae interpolation-based detection and model-based segmentation. *IEEE Trans Med Imaging* 2015; 34: 1649–1662.
- Liu S, Xie Y and Reeves AP. Automated 3D closed surface segmentation: Application to vertebral body segmentation in CT images. *Int J Comput Assist Radiol Surg* 2016; 11: 789–801.
- Kwon SY, Kim JW, Cho MJ, et al. The efficacy of cervical spine phantoms for improving resident proficiency in performing ultrasound-guided cervical medial branch block: A prospective, randomized,

- comparative study. *Medicine (Baltimore)* 2018; 97: e13765.
19. Koo TK and Li MY. A guideline of selecting and reporting intraclass correlation coefficients for reliability research. *J Chiropr Med* 2016; 15: 155–163.
 20. Cohen SL, Schneider R, Carrino JA, et al. Radiation dose practice audit of 6,234 fluoroscopically-guided spinal injections. *Pain Physician* 2019; 22: E119–E125.
 21. Eckel TS and Bartynski WS. Epidural steroid injections and selective nerve root blocks. *Tech Vasc Interv Radiol* 2009; 12: 11–21.